Journal of Applied Polymer Science

Influence of the coupling agent and graphene oxide on the thermal and mechanical behavior of tea dust-polypropylene composites

Pravin Bari, Shital Lanjewar, Dharmesh Parshottam Hansora, Satyendra Mishra
Department of Plastic Technology, University Institute of Chemical Technology, North Maharashtra University, Jalgaon, India
Correspondence to: S. Mishra (Email: profsm@rediffmail.com)

ABSTRACT: In this study, the effects of a coupling agent and additive on the physicomechanical (morphological, mechanical, thermal, and swelling) properties of tea dust (TD)–polypropylene (PP) composites were studied. TD–PP composites were prepared with untreated tea dust (UTD) and tetraethylsilane (TES)-treated TD or silanated tea dust (STD) particles at ratios of 0:100, 10:90, 20:80, 30:70, and 40:60 w/w. Initially, TD particles were grafted by TES as a coupling agent, and these STD particles were then modified with graphene oxide (GO) as an additive to study their effects on the STD–PP composites; these were compared to the STD–PP and UTD–PP composites in accordance with a study of improvements in the mechanical properties. All of the TD–PP composites were analyzed with Fourier transform infrared spectroscopy, scanning electron microscopy, and mechanical, thermal, and physical tests. The thermal and mechanical properties of both the STD–PP and GO-modified STD–PP composites were found to be improved as compared to those of the UTD–PP composites. So, the recycling of a large amount of TD as a waste material could be useful in the preparation of TD–PP composites. © 2015 Wiley Periodicals, Inc. J. Appl. Polym. Sci. **2016**, *133*, 42927.

KEYWORDS: compatibilization; crosslinking; graphene and fullerenes; mechanical properties; nanotubes; thermal properties

Received 25 July 2015; accepted 9 September 2015
DOI: 10.1002/app.42927

INTRODUCTION

Because of the development and growth of technology, natural fibers have been reinforced with a matrix of gluten, starch, and glycerol to produce lightweight and high-strength composite materials.[1,2] The development of natural-fiber-based composite materials is an alternative for environmental and energy concerns.[3–8] Silanated wood flour reinforced in a polypropylene (PP) matrix was reported with improvement in mechanical properties such as the tensile strength (TS) and tensile modulus (TM) of wood–PP composites.[9] Hydrophilic natural fillers adversely affect the adhesion to hydrophobic polymers, and this can change the dimensions of the overall composites. A surface-modified filler can reduce this hydrophilic character and improve the adhesion properties of natural fibers.[10,11] The filler content may also affect the mechanical properties of wood–PP composites.[12] Monticelli *et al.*[13] used different coupling agents for the treatment of fibers and reported that the degree of hydrolysis could enhance the bonding strength of the composite.[14] Silane technology can be used to improve the toughness and creep properties of crosslinked polyethylene–wood flour composites, whereas the noncrosslinked ones showed no such kind of improvement.[15] The bonding strength and adhesion of wood fiber to the polymer matrix can also be increased by the addition of silane coupling agents.[16–18] Higher modulus and tensile and impact strength values of silane-treated cellulose fibers were reported at high loadings of cellulose fibers with a larger size.[19] A reduction in the swelling of water was observed in the case of highly crystalline maleic anhydride treated or maleated PP and maleated wood flour composites having a high weight ratio of flour to PP.[20,21] Other natural and wood fillers, which were treated to develop various polymer composites, for example, agrowaste[22–25] based novolac[22,26,27] and maleated polystyrene,[23,24] high-density polyethylene,[25,28,29] and cane bagasse–melamine formaldehyde.[30] The better crosslinking and uniform dispersion of filler in the PP matrix can be achieved by the surface treatment of the filler.[31,32]

As we know, tea dust (TD) powder is a waste material, especially in urban areas; it is generally not used for any purpose and is discarded as wet garbage.[33] Used particles of TD are advantageous waste materials because they are cheap, light in weight, rich in polyphenols (as tannin present in tea leaves), and easily available from natural resources and a large amount of tea industries and tea stalls. Waste TD materials also have the capability of solving environment-related issues; Hassan *et al.*[34] reported various roles of compatibilizers and their effects on the physicomechanical properties of TD–PP composites and their

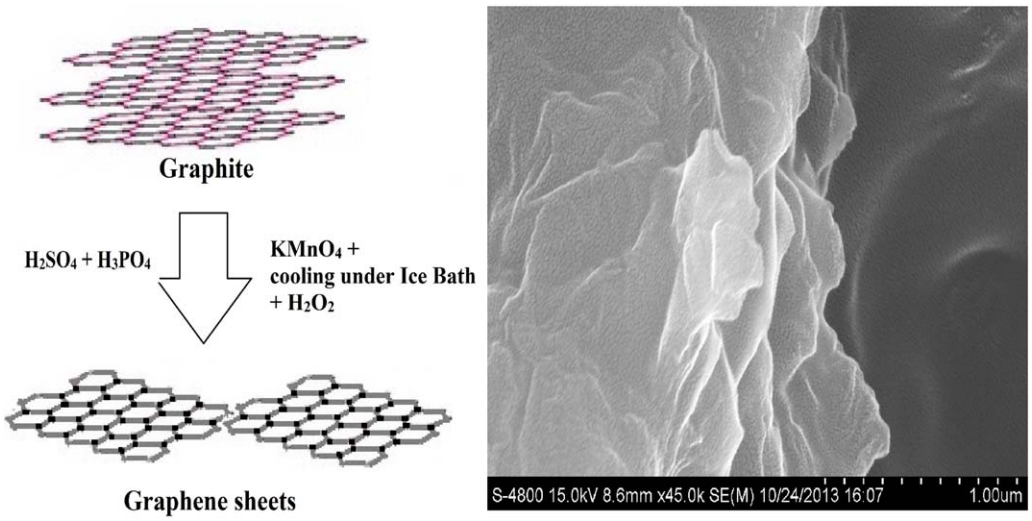

Figure 1. Synthesis steps and surface morphology of GO. [Color figure can be viewed in the online issue, which is available at wileyonlinelibrary.com.]

applications as biocomposites. Ersoy *et al.*[35] investigated the sound absorption of an industrial waste developed during the processing of tea leaves. The biological carbon source present in tea, which has also been found to be useful in the preparation of a cathode material for lithium-ion batteries.[36] Tea-waste-based (magnetite–tea waste) composites have also been reported for the removal of lead ions from the water.[37] Because of green technology and environmental issues, waste TD particles have been used to prepare PP composites as cheap products, especially in building construction sectors.[21,38,39] The use of waste tea leaves has also reported in the production of lactic acid with *Lactobacillus plantarum*.[40] Demir[41] investigated the use of processed waste tea for the production of construction brick. Gatto *et al.*[42] studied the properties of PP composites filled with a mixture of household waste of mate-tea and wood particles. Nevertheless, the use of household waste also increased the properties of the PP composites and showed that it can be a good alternative for the use of renewable materials in the production of polymeric composites.[42]

The introduction of nanomaterials (graphene, metal oxide, metal sulfide, etc.) has prompted the development of conducting polymer nanocomposites[43–46] for emerging applications. In particular, graphene-based nanocomposites have attracted considerable attention because of their unique properties, including their high thermal conductivity, mechanical stiffness, electronic transport properties, and optical and chemical performance.[47–51] Graphene made of atomically thin carbon sheets can also improve the physical properties of host polymers.[52,53] In addition, graphene oxide (GO) is a conducting filler, unlike graphite; this limits its usefulness in the synthesis of conductive nanocomposites.[54] However, a stronger hydration and easier dispersion of GO in water were observed when GO was prepared by the Hummers method.[54–57] GO prepared from graphite flakes can be used on a large scale for the preparation of graphitic films and as a binder for carbon products.[58–60] Carbon nanomaterials such as graphene and GO have been prepared by a modern Hummer's method[42] and the arc-discharge method.[54,61]

On the basis of certain advantages of GO sheets and their composites, we focused on the use of silanated tea dust (STD) and GO-modified STD as organic fillers in commodity–polymer composites; these fillers chemically react and improve their dispersion in the PP matrix. In this study, we also studied the effect of GO on the physicomechanical (morphological, mechanical, and thermal) properties of STD–PP and GO-treated STD–PP composites.

EXPERIMENTAL

Materials

PP (PP-grade ICORENE4014, Icorene Polymers, France), with a melt flow index of 1.5 g/min at 230°C per 2.16-kg load and a density of 0.90 g/cm^3, was used. Acetone, toluene, ether, tetraethylsilane (TES), hydrogen peroxide (H_2O_2), HCl, ethanol, potassium permanganate ($KMnO_4$), sulfuric acid (H_2SO_4), phosphoric acid (H_3PO_4), and methanol were supplied by S.D. Fine Chemicals, Ltd. (Mumbai, India). Graphite powder was received from Merck, Ltd. (Mumbai, India).

Synthesis of GO

Graphite powder (3.0 g) was mixed into a solution of concentrated H_2SO_4 and H_3PO_4 at a 9:1 ratio (360:40 mL). Meanwhile, five to six times the weight of equivalent $KMnO_4$ (18.0 g) powder was also added to graphite mixed solution. This reaction mixture was then heated in a three-necked flask fitted with a water-cooled condenser having a temperature below 50°C and allowed to be stirred continuously for 12 h. The reaction mixture was cooled to room temperature and then kept in an ice bath after the addition of 30% H_2O_2. The resulting suspension was filtered through polyester fiber cloth, and the remaining filtrate was centrifuged at 4000 rpm. The supernatant solution was decanted, and the residual solid material was washed with water, 30% HCl, and finally, ethanol. The solid material was coagulated with 200 mL of ether and vacuum-dried overnight at room temperature. Figure 1 shows the synthesis step and surface morphology of the synthesized GO.

Table I. Compositions of the Filler, Additive, and Polymer

TD as a filler in the polymer matrix (wt %)	PP in the polymer matrix (wt %)	GO as an additive (wt %)	Composition of the STD–PP composite
10	90	0.0	10:90
20	80	0.0	20:80
30	70	0.0	30:70
40	60	0.0	40:60
40	60	0.5	40:60/0.5 wt %
40	60	1.0	40:60/1.0 wt %
40	60	1.5	40:60/1.5 wt %
40	60	2.0	40:60/2.0 wt %

Silane Treatment of the TD Particles

TD is generally composed of moisture, ash, lignin, cellulose, hemicellulose, and flying material. The used particles of TD were collected from the tea stalls, initially washed with water, followed by acetone to remove the traces of water, and then dried and ground in a mortar and pestle to a 35-mesh size to obtain untreated tea dust (UTD) particles. A 10 g of TD was treated with 2 mL of TES as a commercial compatibilizer in 100 mL of toluene and then allowed to reflux for 1 h followed through drying at room temperature for 30 min. This treated material is called STD in the text.

Preparation of the TD–PP Composites

GO solutions of 0.5, 1.0, 1.5, and 2.0 g in 50 mL of acetone were prepared individually by mixing under ultrasonic treatment for 10 min. These different GO solutions were individually mixed with STD, and then, we allowed the excess acetone to evaporate from the resulting GO–STD solution mixtures. UTD and STD were weighed precisely and mixed with the commodity polymer PP at different weight ratios:[34] 10:90, 20:80, 30:70, and 40:60 w/w. The predetermined weight ratios of UTD–PP, STD–PP, and GO-treated STD–PP composites were mixed properly in an injection-molding machine before the mechanical tests according to American Society for Testing and Materials (ASTM) standards. Thereafter, we fed the mixed material into an injection-molding machine by keeping the temperatures of the feed, compression, and metering zones at 150, 170, and 180°C, respectively. The mold temperature was initially kept at 30°C, whereas the molding process was carried out at 150–180°C and then allowed to mix for a duration of 15 min with a compression pressure of 3 MPa.[42] Direct contact between the PP powder and metal platens during the heating and pressing process occurred, and greasy paper was used for proper separation. The specimens of all of the TD–PP composites were cut out with dimensions of 6.4 × 1.25 × 0.21 cm^3. Table I shows different compositions of UTD–PP, STD–PP, and GO-modified STD–PP composites with their relative amounts (in weight percentage) of filler, additive, and polymer.

Characterization

Fourier Transform Infrared (FTIR) Spectroscopy. Samples of UTD, STD, and GO-modified STD were finely divided and dispersed in KBr powder for analysis. An FTIR spectrophotometer (8400, Shimadzu, Tokyo, Japan) was used to obtain the spectra of UTD and STD, to understand the bond formation due to the surface treatment, and to judge the composites for their resistivity to water. A total of 45 scans were taken for all of the composite samples; they were recorded at 4000–400 cm^{-1} with a resolution of 4 cm^{-1} in transmittance mode.

Scanning Electron Microscopy (SEM). Morphological studies were carried out on a scanning electron microscope (S4800, Type II, Hitachi, Tokyo, Japan) at an operation voltage of 10 keV and a pressure of 1.33 g/cm^2. All of the TD–PP composites were gold-coated to make them conductive, and they were mounted on the specimen tube before they were viewed with SEM.

X-ray Diffraction (XRD). XRD spectra were obtained on an X-ray diffractometer (D8, Bruker, Coventry, Germany) with Cu $K\alpha_1$ radiation ($\lambda = 1.5404$ Å) within the 2θ range 20–80° and operated at a voltage of 40 keV and with a current of 40 mA. A dwell time of 2 s per step was used. The crystalline phases and their relative contents in materials were quantitatively obtained by location and the number of diffraction peak and relative intensity of the XRD pattern.

Mechanical Properties. Tensile tests were carried out as per ASTM D 638 on a universal testing machine (UTM) (Instron 5582, Buckinghamshire, United Kingdom) at a speed of 0.4 cm/min with a span length of 0.4 cm and a load of 500 kg. Flexural tests were carried out per ASTM D 790 on a UTM machine (Dipak Polyplast Private Limited 484, Ahmedabad, India). The impact strength was determined per ASTM D 256 with an Izod impact tester (Polyplast Equipment, Mumbai, India, falling weight = 293) with a notched specimen. The specimen having predetermined dimensions was clamped at the specimen holder, and then, it was subjected to sudden shock with a hammer. Hardness tests were also performed on a Shore-D hardness tester (ASTM D 2240). The hardness test was carried out by the placement of a specimen on a hard, flat surface. The pressure foot of the instrument was pressed onto the specimen to make sure that it was parallel to the surface of the specimen, and the hardness was read as it was displayed. All of the tests were

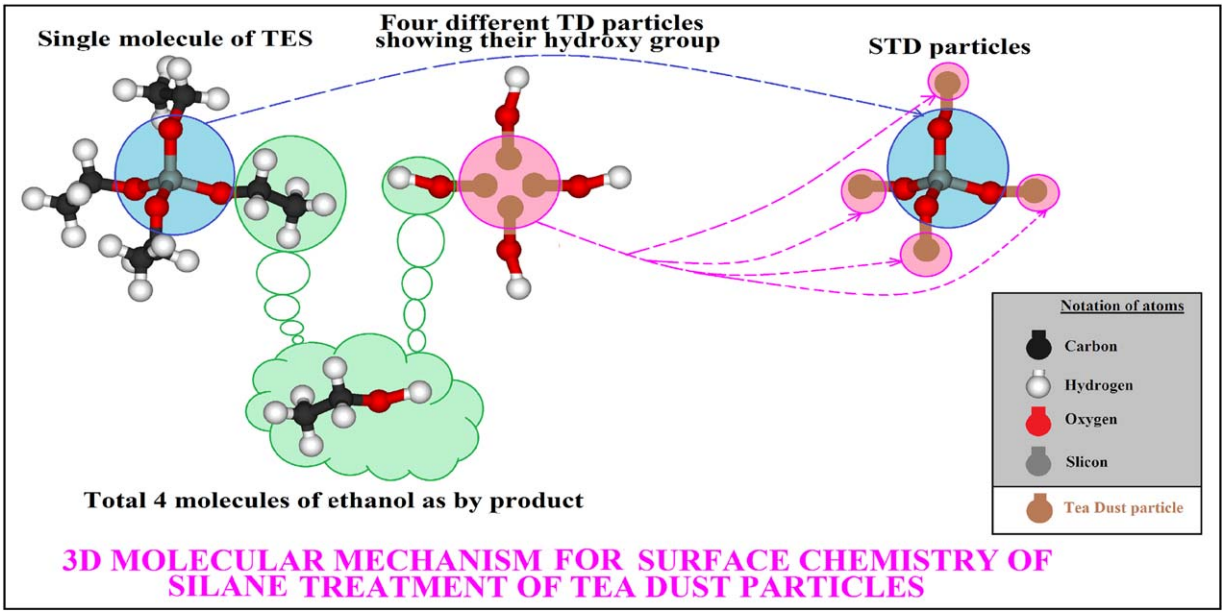

Figure 2. Surface chemistry of the silane treatment of TD particles (3D = three-dimensional). [Color figure can be viewed in the online issue, which is available at wileyonlinelibrary.com.]

repeated five times, and the mean values of the results were reported in the text.

Thermal Properties. The Vicat softening temperature (VST) was recorded on a Vicat softening tester (Shant Engineering, Mumbai, India) according to the standards set forth in ASTM D 1525 with a standard load of 1 kg and a heating rate of 2 ± 0.2°C/min.[62] This VST test was carried out by the placement of the test sample on a specimen support and the lowering of the needle rod so that the needle could rest on the surface of the specimen. The temperature of the bath was increased uniformly at a rate of 50°C/h. The temperature at which the needle penetrated about 1 mm deep was recorded as the VST. The differential scanning calorimetry (DSC) was carried out on a differential scanning calorimeter (DSC 60, Shimadzu, Tokyo, Japan) for the study of the UTD–PP, STD–PP, and GO-modified STD–PP composites. A sample of 5–7 mg was taken and sealed in an aluminum pan before DSC measurement. The peak temperature and change in enthalpy (ΔH) were obtained from the maxima and area of the melting peak, respectively.

RESULTS AND DISCUSSION

Confirmation of the Silane Treatment of the TD Particles

Figure 2 shows the molecular chemistry mechanism of the treated surfaces of the TD, TES, and STD particles. As shown during the silane treatment of the TD particles, ethyl (CH_3CH_2—) groups present in TES reacted with the hydroxyl (—OH) groups of the TD particles because STD containing polar hydroxyl groups (—OH) are helpful for improving their dispersion in the PP composite matrix. As there are total four ethyl groups present in TES that can react easily with four different TD particles (as shown in Figure 2) to produce STD particles and also generate four molecules of ethanol as a byproduct. In addition, STD has a polar and long-silane-treated TD chain (4TD-SiO_4), as shown in the molecular (Figure 2) structure; this helped to improve the mechanical performance of the TD–PP composites.

We confirmed from the FTIR spectra the presence of silicate stretching at 921.04 cm^{-1}, silicone bonding at 1238.34 cm^{-1}, ethoxy group at 1442.8 cm^{-1} of silane, and C=C stretching at 1650.16 cm^{-1} (Figure 3).[15–19] These vibrations were absent in UTD, as also shown in Figure 3; this suggested the proper functionalization by TES over the surface of the TD particles.

Morphological Properties

Figure 4(a–c) shows SEM micrographs of the pure PP and UTD–PP and STD–PP composites, respectively. The UTD–PP

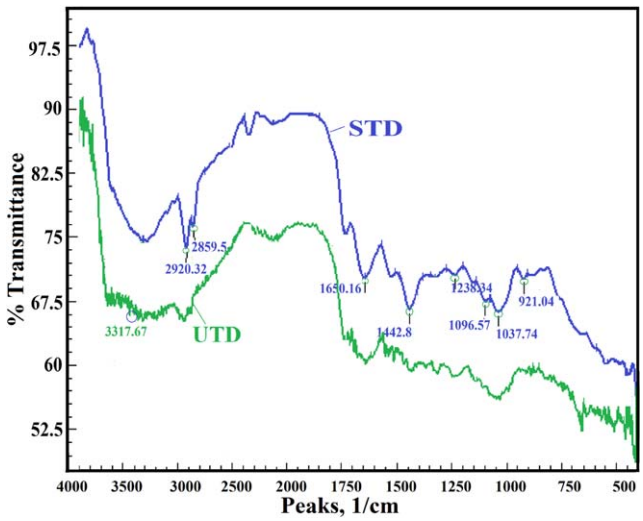

Figure 3. FTIR spectra of the untreated and silane-treated TD. [Color figure can be viewed in the online issue, which is available at wileyonlinelibrary.com.]

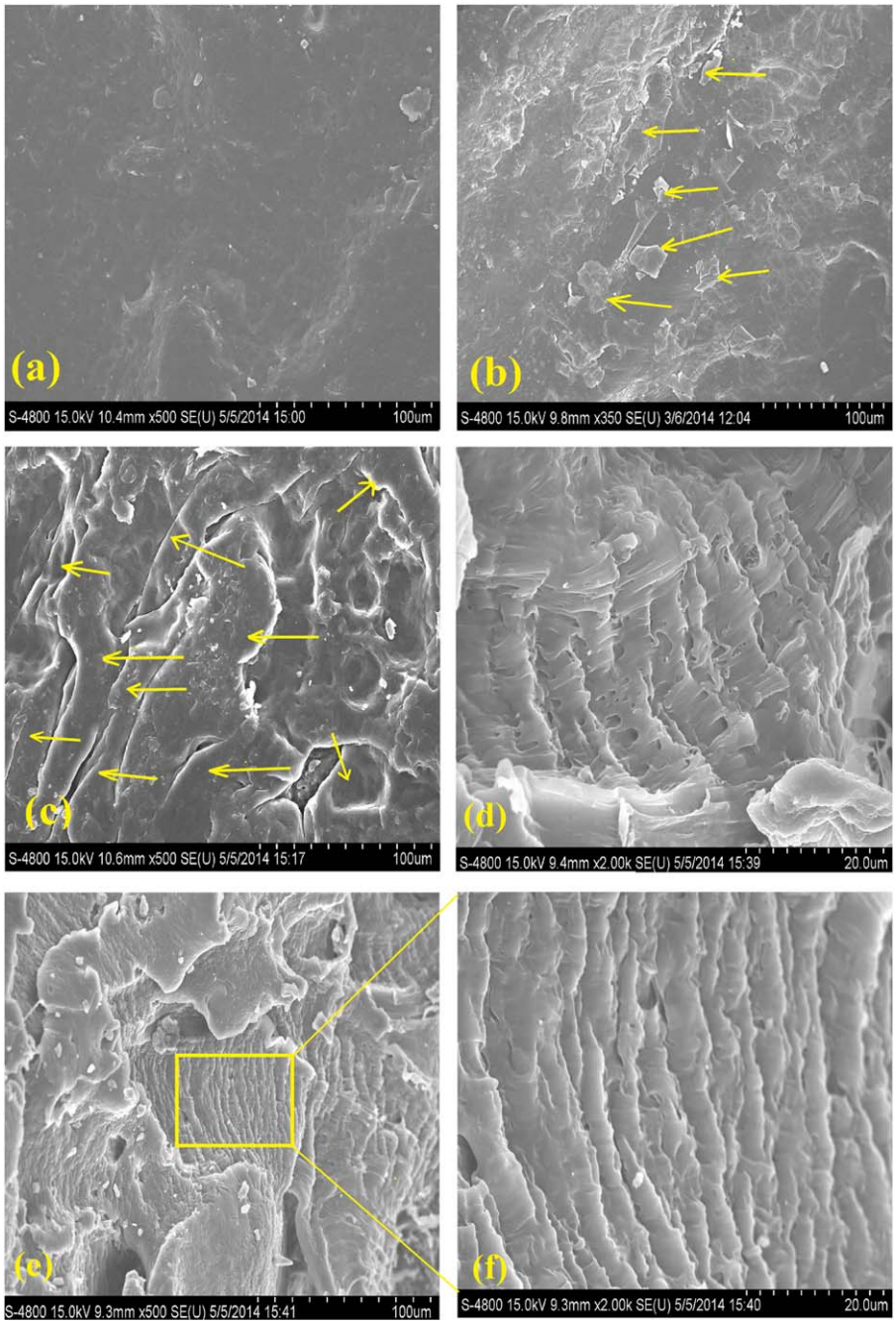

Figure 4. FESEM micrographs: (a) PP, (b) UTD–PP and (c) STD–PP composites, and STD–PP composites modified by (d) 1 wt % GO and (e,f) 2 wt % GO. [Color figure can be viewed in the online issue, which is available at wileyonlinelibrary.com.]

composites showed agglomeration because of the uneven distribution of filler; this affected the mechanical and physical properties of the composites. As shown in Figure 4(c), there was no clear cleft between the matrix and fillers; this indicated good interfacial bonding between them. This also indicated a uniform dispersion of STD particles into the PP matrix; this was better compared to the UTD–PP composites because of the TES treatment on the surface of the TD particles. Thus, adhesion between the STD and PP matrix in the composite became better than that of UTD one; this is shown clearly in Figure 4(b). In addition, the surface morphology showed that the treated STD filler was utterly attached and strongly imbedded in the PP matrix; this indicated better efficiency of mixing and was attributed to a good interfacial interaction between the hybrid filler and the polymer matrix. This was also strengthened by the results reported by Hamid *et al.*[63] The interfacial bonding was improved because of the ethoxy treatment. This meant that stress was well propagated between the filler and polymer matrix; this resulted in enhanced TS and TM values in response to stress.[64]

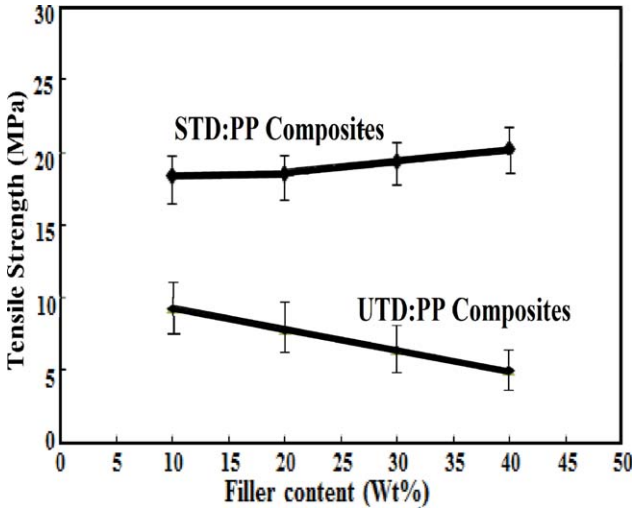

Figure 5. TSs of the TD–PP composites. [Color figure can be viewed in the online issue, which is available at wileyonlinelibrary.com.]

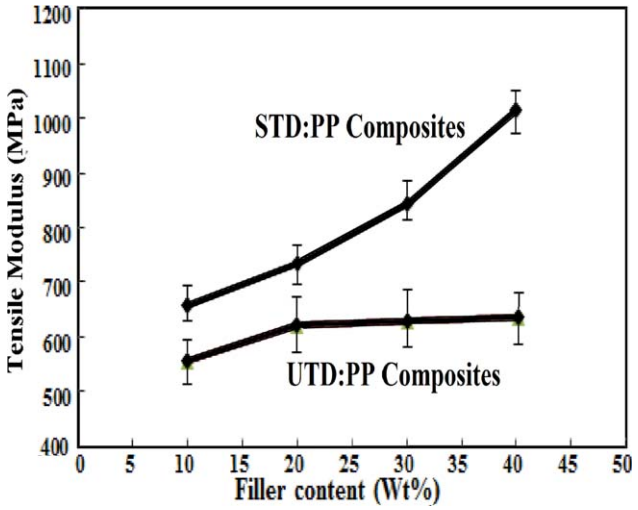

Figure 6. TMs of the TD–PP composites. [Color figure can be viewed in the online issue, which is available at wileyonlinelibrary.com.]

In comparison to STD–PP (40:60), the GO-modified STD–PP (40:60) composites were more uniform with a continuous overlap of layered structures [Figure 4(d,f)]; this was due to the proper dispersion and the presence of GO sheets in the STD–PP composites, which directly affected the properties of the STD–PP (40:60) composites. An improvement in the compatibility between the PP matrix and STD filler was also visualized, and this was confirmed by FTIR spectra (Figure 3) and field emission scanning electron microscopy (FESEM) micrographs (Figure 4). The filler became nonpolar in nature because of the surface treatment, and hence, this improved the compatibility between PP and STD. As a result, STD formed a bond with the PP matrix. Figure 2 shows the detailed mechanism; it indicates that the TES esterified free hydroxyl (—OH) groups present in the TD particles.

Mechanical Properties

TS, TM, and Flexural Strength (FS). The effects of various TD contents (10, 20, 30, and 40 wt %) on the different mechanical properties of the TD–PP composites were studied. We observed in Figure 5 that TS decreased with increasing filler contents from 10–40 wt % in the UTD–PP composites, whereas the STD–PP composites showed an increasing trend. TS increased with increasing filler content and showed an almost double value (20 MPa) for the STD–PP (40:60) composites and a more than double value (20.7 MPa) for the GO-modified STD–PP composites compared to those of the UTD–PP composite, which had a minimum TS (<10 MPa). A sufficient STD content in PP increased the TS of the composites. At lower STD contents, the composites showed low TSs because of the poor filler content and low load-transfer capacity to one another. More importantly, virgin PP showed a higher TS (24 MPa) compared to the UTD–PP and STD–PP composites.

Unlike TS, with an increase in the TD content in the PP composites, TM also showed an increasing trend for both the UTD–PP and STD–PP composites, as shown in Figure 6. TM also increased with increasing filler content and showed values nearer to double for both the STD–PP (40:60) composites (1014 MPa) and GO-modified STD–PP composites (1044 MPa) as compared to that of the UTD–PP composite, which had a minimum TM (~550 MPa). However, TM of the virgin PP was reported to be the maximum at about 2200 MPa. From the previous interpretation and according to the TS and TM values (Table II), the optimized content of STD (i.e., GO-modified STD) in the PP matrix composites was 40 wt %; this showed a

Table II. Mechanical Properties of the GO-Modified STD–PP Composites

Composition of the STD-PP composites modified by GO	Mechanical properties of the GO-modified STD-PP composites				
	TS (MPa)	TM (MPa)	FS (MPa)	IS (J/m)	Hardness
40:60	20.2	1014	1014	32	68
40:60/0.5 wt %	20.3	1017	1017	30	69
40:60/1.0 wt %	20.4	1025	1025	30	70
40:60/1.5 wt %	20.5	1038	1038	29	70
40:60/2.0 wt %	20.7	1044	1045	28	71

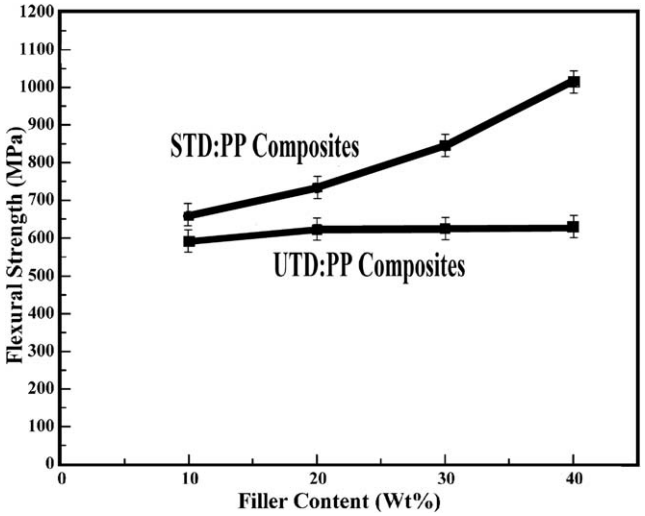

Figure 7. FSs of the TD–PP composites.

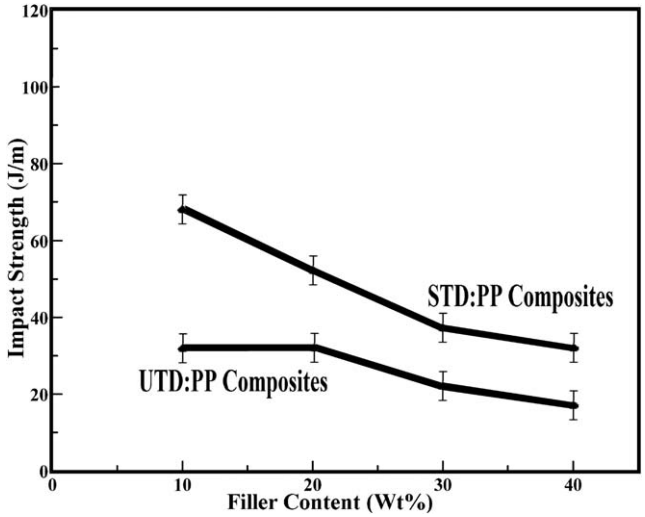

Figure 8. ISs of the TD–PP composites.

significant improvement in the mechanical performance, with a TS of 20.7 MPa and a TM of 1044 MPa. These results were in accordance with those of Stark and Berger.[65]

As shown in Figure 7, FS increased with increasing TD content from 10 to 40 wt % of both UTD and STD. FS of the UTD–PP (40:60) composite was recorded as 628 MPa, whereas that of the STD–PP (40:60) composites was 1014 MPa; this was an improvement of about 61%. This clearly indicates that the greater FS of STD–PP (40:60) compared to the UTD one was due to the enhancement of the tension transference of the filler–polymer interface, which resulted from the compatibilization of TD with the PP matrix, which resulted from the silane treatment of the filler.[20] Table II shows FS of the GO-modified STD–PP composites; this shows that the values of FS marginally increased as the GO content increased from 0.5 to 2 wt %. The maximum value (1045 MPa) of FS was recorded for the 2 wt % GO-modified STD–PP (40:60) composites; this was 66% higher than that of the UTD–PP composites (FS = 1014 MPa). Also, the virgin PP had a higher value of FS of about 1090 MPa.

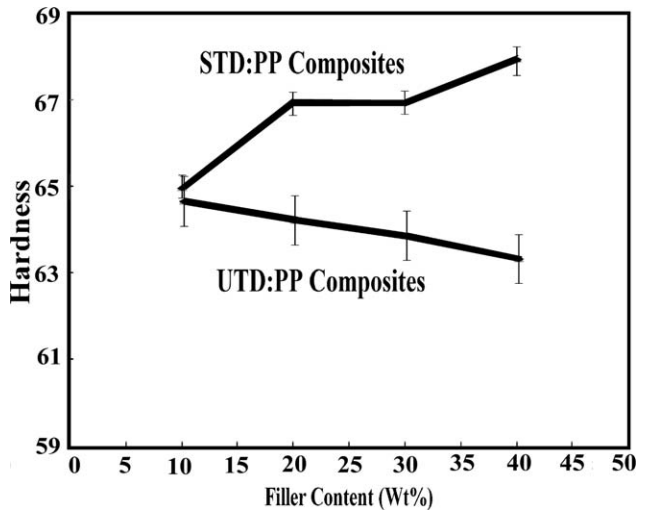

Figure 9. Hardness values of the TD–PP composites.

Impact Strength and Hardness. The decreasing trend of the impact strength (IS) was clearly observed, as shown in Figure 8. This decrement was with respect to the increase in both the UTD and STD contents in the respective PP composites; however, the range of IS of UTD–PP was greater (17–32 J/m) than that of STD one (32–68 J/m) in all cases. The highest value for IS was recorded as 68 J/m in the case of the STD–PP (10:90) composites, whereas the value was 103 MPa in the case of the virgin PP. The lowest value of IS (28 J/m) was observed for the 2 wt % GO-modified composite. The decreasing trend was also observed for the IS of the GO-modified STD–PP composites with increasing GO content; however, the IS of the unmodified STD–PP was greater than that of the GO-modified STD–PP composites (Table II).

Opposite trends for the hardness of both the UTD–PP and STD–PP composites are clearly shown in Figure 9. The hardness

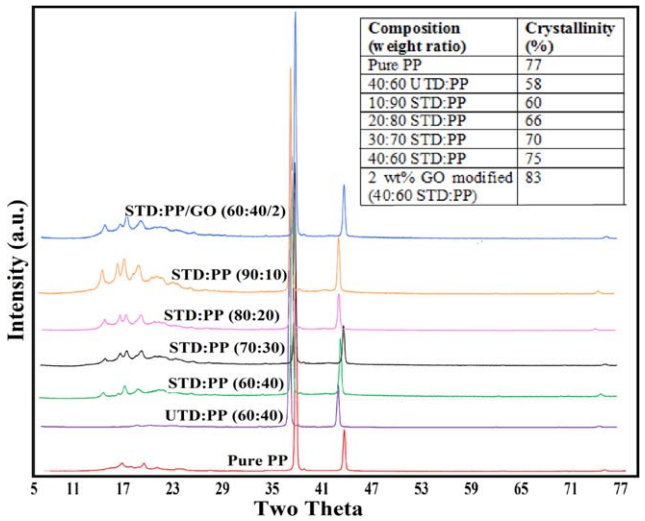

Figure 10. XRD patterns of the virgin PP, UTD–PP and STD–PP composites, and STD–PP (40:60) composites modified by 2 wt % GO. [Color figure can be viewed in the online issue, which is available at wileyonlinelibrary.com.]

Table III. Thermal Behavior of the TD–PP Composites

Composition (weight ratio)	Temperature (°C)		ΔH (J/gm)
	Endothermic peak	Degradation	
Pure PP	169	150	−4.06
UTD–PP (40:60)	169	468	−1.60
STD–PP (10:90)	164	376	−2.12
STD–PP (20:80)	165	375	−2.55
STD–PP (30:70)	167	403	−3.25
STD–PP (40:60)	168	410	−4.60
2 wt % GO-modified STD–PP (40:60)	166	452	−3.40

of the UTD–PP composites indicated a decreasing order and that of the STD–PP composites showed an increasing order with increasing filler contents from 10 to 40 wt % in the respective composites. The virgin PP had a hardness of 68, whereas the hardness of the 2 wt % GO-modified STD–PP (40:60) composites increased from 68 to 71 with increasing GO content (Table II).

An increment in the hardness of the GO-modified STD–PP composites was also observed; this was with respect to the increase in the GO content in the composites. This increment was due to the increase in the crystallinity values, which were recorded as 58, 75, and 83 for the UTD–PP, STD–PP, and 2 wt % GO-modified STD–PP (40:60) composites, respectively (Figure 10). The surface modification of the TD particles with TES increased the crosslinking bonds between the TD particles and the commodity polymer. Moreover, GO itself was a crystalline material, and virgin PP also had a higher (~77%) crystallinity. As a result, the change in crystallinity (43% improvement), which was significant, of the 2 wt % GO-modified STD–PP composites could have been related to the mechanical properties. The GO-modified STD–PP composites had more uniform

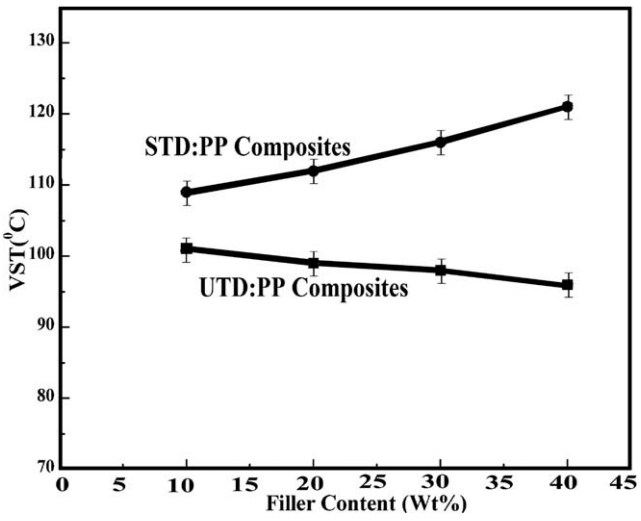

Figure 11. VSTs of the (a) UTD–PP and (b) STD–PP composites.

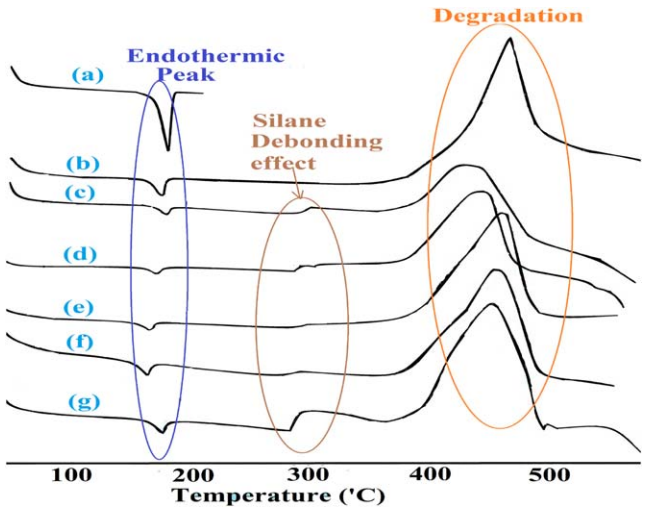

Figure 12. DSC thermograms of the (a) PP and (b) 40:60 UTD–PP, (c) 10:90 STD–PP, (d) 20:80 STD–PP, (e) 30:70 STD–PP, (f) 40:60 STD–PP, and (g) 40:60 STD–PP composites modified by 2 wt % GO. [Color figure can be viewed in the online issue, which is available at wileyonlinelibrary.com.]

layered and continuously overlapped structures, as shown clearly in the FESEM micrographs (Figure 4). However, in the case of the UTD–PP composites, poor adhesion between the matrix and hybrid fibers generated void space at the interface of the polymer-filler; this led to a lower IS in the TD–PP composites, as reported in our earlier work.[66]

Thermal Properties

Thermal (VST and DSC) studies of the UTD and STD–PP composites were carried out to understand the effect of the filler compatibility on the thermal behavior of the PP composites. We observed from the VST results (Figure 11) that VST decreased with increasing UTD content in the PP matrix; the values recorded were 101, 98.6, 97.5, and 96°C, whereas in the case of the STD–PP composites, these values were recorded as 109, 112, 116, and 121 for 10, 20, 30, and 40 wt % UTD and STD contents, respectively. The main findings of household-mate-tea-waste-based PP composites were the decrease (from 101 to 96°C) in the thermal stability of UTD–PP and the increase (from 109 to 121°C) in that of the STD–PP composites from virgin PP (VST = 68°C); this was also reported by Mattos *et al.*[42] and Mishra *et al.*[20]

Table III and Figure 12 show the thermal behavior of the PP, UTD–PP, and STD–PP composites. We observed from the results that there was not much variation in the onset, end set, and peak temperatures of the TD–PP composites. However, the changes in enthalpy were reported as −4.06, −1.6, −4.60, and −3.4 J/g for the PP and UTD–PP (40:60), STD–PP (40:60), and 2 wt % GO-modified STD–PP (40:60) composites, respectively. These results show an increasing endothermic trend with increasing amount (up to 40 wt %) of STD in the PP composites. We also observed that the debonding of the silane treatment occurred above 285°C in the STD–PP composites. However, this effect was more pronounced in the GO-modified STD–PP composite (Figure 12).

When the results of the UTD–PP (40:60) composite were compared with those of the STD–PP (40:60) composites, the heat flow of the treated (STD–PP) one was greater. These results were also strengthened by XRD analysis, which showed the crystallinity values reported in Figure 10 and those described previously. The degradation temperature for the GO-modified STD–PP composites was at a maximum of 452°C; this was approximately 42°C higher than that of the STD–PP composites. However, the maximum degradation temperature of the UTD–PP was recorded as 468°C. This reduction in the degradation temperature of STD–PP was due to the debonding of silane, whereas in case of the GO-modified STD–PP composite, the GO itself provided better thermal stability because of its endothermic nature.

CONCLUSIONS

All of the TD–PP composites were successfully prepared on an injection-molding machine with various TD contents from 10–40 wt %. The thermal, mechanical, and physical properties of the UTD–PP composites decreased with increasing filler content. However, after the treatment of TES, the compatibility of the TES-treated TD (STD) with PP increased, and all of these increments in the physicomechanical properties of the STD–PP composites as compared to the UTD ones were observed.

In this study, optimum compatibilization and, therefore, better mechanical properties within the PP composite were observed for the 2 wt % GO-modified STD–PP (40:60) composites. The TS of the GO-modified STD–PP composites was significantly improved (almost double) compared to that of the UTD–PP one. Compared to the UTD–PP (40:60) composites, the TM and FS values of the 2 wt % GO-modified STD–PP composites were about 89 and 66% improved. The IS of STD–PP was recorded as 68 J/m; this was more than double compared to that of the 2 wt % GO-modified STD–PP and UTD–PP composites. The hardness of the 2 wt % GO-modified STD–PP composites was improved by 14.5% compared to that of the UTD–PP one. The degradation temperature for the 2 wt % GO-modified STD–PP composites was 42°C higher than that of the unmodified STD–PP composites. An endothermic trend was observed for the STD–PP composites as the filler content increased. There was a 43% improvement in the crystallinity of the 2 wt % GO-modified STD–PP composites compared to that of the UTD–PP one. So, the overall thermal, mechanical, and physical properties of the 2 wt % GO-modified STD–PP (40:60) composites were found to be improved, and these composites can be suggested for suitable engineering materials in building and construction sectors and for industrial applications.

ACKNOWLEDGMENTS

The authors are thankful to the National Project Implementation Unit, the Ministry of Human Resource Development, and the University Grants Commission (New Delhi, India) for providing financial assistance through a grant (University Grants Commission/Basic Scientific Research project F.4-10/2010; September 20, 2011) to perform this research work.

REFERENCES

1. Rout, J.; Misra, M.; Mohanty, A. K.; Nayak, S. K.; Tripathi, S. S. *J. Reinf. Plast. Compos.* **2003**, *22*, 1083.
2. Corradini, E.; de Morais, L. C.; de Rosa, F. M.; Mazzetto, S. E.; Mattoso, L. H. C.; Agnelli, J. A. M. *Macromol. Symp.* **2007**, *1*, 558.
3. Geethamma, V. G. *Polymer* **1998**, *39*, 1483.
4. Satyanarayana, K. G.; Sukumaran, K.; Mukherjee, P. S.; Pavithran, C.; Pillai, S. G. K. *J. Cem. Concr. Compos.* **1990**, *12*, 117.
5. Satyanarayana, K. G.; Sukumaran, K.; Kulkarni, A. G.; Pillai, S. G. K.; Rohatgi, P. K. *J. Compos.* **1986**, *17*, 329.
6. Nabisaheb, D.; Jog, J. P. *Adv. Polym. Technol.* **1999**, *18*, 351.
7. Herrera-Franco, P. J.; González-Valadez, A. *Compos. B* **2005**, *36*, 597.
8. Tungjitpornkull, S.; Sombatsompop, N. J. *Mater. Process. Technol.* **2009**, *209*, 3079.
9. Ichazo, M. N.; Albano, C.; González, J.; Perera, R.; Candal, M. V. *Compos. Struct.* **2001**, *54*, 207.
10. Mishra, S.; Naik, J. B. *Compos. Sci. Technol.* **2000**, *60*, 1729.
11. Naik, J. B.; Mishra, S. *Polym. Plast. Technol. Eng.* **2006**, *45*, 927.
12. Zaini, M. J.; Fuad, M. Y.; Ismail, Z.; Mansor, M. S.; Mustafah, J. *Polym. Int.* **1996**, *40*, 51.
13. Montecelli, F.; Toledano, M.; Osorio, R.; Ferrari, M. *Dent. Mater.* **2006**, *22*, 1024.
14. Standard Test Methods for Evaluating Properties of Wood Base Fiber and Particle Panel Material; ASTM D 1037-12. DOI: 10.1520/D1037-12. http://www.astm.org/Standards/D1037.htm Accessed on October 15, **2013**.
15. Bengtsson, M.; Oksman, K. *Compos. A* **2006**, *37*, 752.
16. Razi, P.; Portier, R.; Raman, A. *J. Compos. Mater.* **1999**, *33*, 1064.
17. Nourbakhash, A.; Karegarfard, A.; Ashori, A. *J. Thermoplast. Compos. Mater.* **2010**, *23*, 169.
18. Elvy, S. B.; Dennis, R. G.; Loo-Teck, N. *J. Mater. Process. Technol.* **1995**, *48*, 365.
19. Abdelmouleh, M.; Boufi, S.; Belgacem, M. N.; Dufresne, A. *Compos. Sci. Technol.* **2007**, *67*, 1627.
20. Mishra, S.; Verma, J. *Polym. Plast. Technol. Eng.* **2006**, *45*, 1199.
21. Mishra, S.; Verma, J. *J. Appl. Polym. Sci.* **2006**, *101*, 2530.
22. Mishra, S.; Naik, J. B. *J. Appl. Polym. Sci.* **1998**, *68*, 681.
23. Mishra, S.; Naik, J. B. *J. Appl. Polym. Sci.* **1998**, *68*, 1417.
24. Mishra, S.; Naik, J. B. *Polym. Plast. Technol. Eng.* **2005**, *44*, 663.
25. Mishra, S.; Naik, J. B. *Polym. Plast. Technol. Eng.* **2005**, *44*, 511.
26. Mishra, S.; Patil, Y. P. *J. Mol. Cryst. Liq. Cryst.* **2004**, *418*, 101.
27. Patil, Y. P.; Gajare, B.; Dusane, D.; Chavan, S.; Mishra, S. *J. Appl. Polym. Sci.* **2000**, *77*, 2963.

28. Naik, J. B.; Mishra, S. *Polym. Plast. Technol. Eng.* **2005**, *44*, 687.
29. Naik, J. B.; Mishra, S. *J. Appl. Polym. Sci.* **2007**, *106*, 2571.
30. Mishra, S.; Patil, Y. P. *J. Appl. Polym. Sci.* **2003**, *88*, 1768.
31. George, J.; Sreekala, M.; Thomas, S. *Polym. Eng. Sci.* **2001**, *41*, 1471.
32. Eichhorn, S. J.; Baillie, C. A.; Zafeiropoulos, N.; Mwaikambo, L. Y.; Ansell, M. P.; Dufresne, A.; Entwistle, K. M.; Herrera-Franco, P. J.; Escamilla, G. C.; Groom, L.; Hughes, M.; Hill, C.; Rials, T. G.; Wild, P. M. *J. Mater. Sci.* **2001**, *36*, 2107.
33. Gurav, M.; Sinalkar, S. In Proceedings of National Conference on Biodiversity: Status and Challenges in Conservation - 'FAVEO' 2013; 2013; p 97. ISBN 978-81-923628-1-6. http://www.vpmthane.org/sci/FAVEO/r14.pdf
34. Hassan, M. M.; Mueller, M.; Tartakowska, D. J.; Wagner, M. H. *J. Appl. Polym. Sci.* **2012**, *125*, E413.
35. Ersoy, S.; Cu, K.; Ku, H. *Appl. Acoust.* **2009**, *70*, 215.
36. Wei, C.; He, W.; Zhang, X.; Liu, S.; Jin, C.; Liu, S.; Huang, Z. *RSC Adv.* **2015**, *5*, 28662.
37. Yeo, S. Y.; Choi, S.; Dien, V.; Peh, Y. K. S.; Qi, G.; Hatton, T. A.; Doyle, P. S.; Joo, B.; Thio, R. *PLoS One* **2013**, *8*, e66648.
38. Mueller, D. H.; Krobjilowski, A. *J. Ind. Text.* **2003**, *33*, 111.
39. Bledzki, A. K.; Gassan, J. *Prog. Polym. Sci.* **1999**, *24*, 221.
40. Gowdhaman, D.; Sugumaran, K. R.; Ponnusami, V. *Int. J. Chem. Technol. Res.* **2012**, *1*, 143.
41. Demir, I. *Build. Environ.* **2006**, *41*, 1274.
42. Mattos, B. D.; Misso, A. L.; de Cademartori, P. H. G.; de Lima, E. A.; Magalhaes, W. L. E.; Gatto, D. A. *Construct. Build. Mater.* **2014**, *61*, 60.
43. Rana, V. K.; Choi, M. C.; Kong, J. Y.; Kim, G. Y.; Kim, M. J.; Kim, S. H.; Mishra, S.; Singh, R. P.; Ha, C. S. *Macromol. Mater. Eng.* **2011**, *296*, 131.
44. Rana, V. K.; Akhtar, S.; Chatterjee, S.; Mishra, S.; Singh, R. P.; Ha, C. S. *J. Nanosci. Nanotechnol.* **2014**, *14*, 2425.
45. Shimpi, N. G.; Mali, A. D.; Hansora, D. P.; Mishra, S. *Nanosci. Nanoeng.* **2015**, *3*, 8.
46. Yeole, B.; Sen, T.; Hansora, D. P.; Mishra, S. *J. Appl. Polym. Sci.* **2015**, *132*, 42379.
47. Kim, H.; Abdala, A. A.; Macosko, W. C. *Macromolecules* **2010**, *43*, 6515.
48. Sun, Y.; Shi, G. *J. Polym. Sci. Part B: Polym. Phys.* **2013**, *51*, 231.
49. Hu, K.; Kulkarni, D. D.; Choi, I. *Prog. Polym. Sci.* **2014**, *39*, 1934.
50. Chen, W. D.; Weng, W.; Cuiling, W. *Carbon* **2003**, *41*, 619.
51. Hummers, W. S.; Offeman, R. E. *J. Am. Chem. Soc.* **1958**, *80*, 1339.
52. Rodil, S. V. *J. Mater. Chem.* **2009**, *19*, 3591.
53. Chen, T.; Zeng, B. Q.; Liu, J. L.; Dong, J. H.; Liu, X. Q.; Wu, Z.; Yang, X. Z.; Li, Z. M. *J. Phys. Conf. Ser.* **2009**, *188*, 012051.
54. Hansora, D. P.; Shimpi, N. G.; Mishra, S. *JOM* **2015**, 1. DOI: 10.1007/s11837-015-1522-5.
55. You, S.; Luzan, S. M.; Szabo, T.; Talyzin, A. V. *Carbon* **2013**, *52*, 171.
56. Kotov, N. A.; Dekany, I.; Fendler, J. H. *Adv. Mater.* **1996**, *8*, 637.
57. Du, X. S.; Xiao, M.; Meng, Y. Z. *Synth. Met.* **2004**, *143*, 129.
58. Ishikawa, T.; Nagaoki, T.; Kogyo, S. T. New Carbon Industry, 2nd ed.; Kindai Hensyusya: Tokyo, **1986**; p 125.
59. Touzain, P.; Yazumi, R.; Maire, J. U.S. Pat. 4584,252. **1986**.
60. Jung, I.; Dikin, D. A.; Piner, R. D.; Ruoff, R. S. *Nano Lett.* **2008**, *8*, 4283.
61. Shimpi, N. G.; Mishra, S.; Hansora, D. P.; Savdekar, U. Indian Pat. 3179/MUM/2013 (2013). http://ipindia.nic.in/ipr/patent/journal_archieve/journal_2013/pat_arch_102013/official_journal_25102013_part_i.pdf. Accessed on April 28, **2015**.
62. Shah, V. Handbook of Plastics Testing Technology; Wiley: New York, **1951**; p 90.
63. Hamid, M. R. Y.; Ab Ghani, M. H.; Ahmad, S. *Ind. Crops Prod.* **2012**, *40*, 96.
64. Chen, H. C.; Chen, T. Y.; Hsu, C. H. *Eur. J. Wood Prod.* **2006**, *64*, 172.
65. Stark, N.; Berger, M. In Proceedings: Functional Fillers for Thermoplastics & Thermosets, San Diego, CA, 1997; USDA Forest Service, Forest Products Laboratory: Madison, WI, **1997**; p 1.
66. Mishra, S.; Naik, J. B.; Patil, Y. P. *Adv. Polym. Technol.* **2004**, *23*, 46.